**Indonesian Journal of Electrical Engineering and Computer Science**
Vol. 42, No. 3, June 2026, pp. 786~797
ISSN: 2502-4752, DOI: 10.11591/ijeecs.v42.i3.pp786-797 

# Adaptive fractional-order PID-controlled DVR optimized by zebra algorithm for harmonic suppression

**Milind Paraye, Rajendra G. Sutar**
Department of Electronics and Telecommunication Engineering, Sardar Patel Institute of Technology, University of Mumbai, Mumbai, India

**Article Info**

***Article history:***

Received Aug 1, 2025
Revised Mar 12, 2026
Accepted May 28, 2026

***Keywords:***

DVR
Grid-connected systems
Power quality
Total harmonic distortion
Voltage sag
Voltage stability

**ABSTRACT**

Dynamic voltage restorers (DVRs) are widely employed to mitigate power quality disturbances in modern power grids. Existing DVR control strategies frequently struggle to adequately suppress harmonic distortions and voltage sags due to nonlinear grid behaviour, rapidly varying disturbances, and limited tuning flexibility. We suggest a grid-connected DVR with an adaptive fractional order proportional integral derivative (FOPID) controller whose parameters are improved using an improved zebra algorithm (IZA) in order to close this gap. The IZA algorithm is used to improve the FOPID controller parameters, ensuring rapid convergence and superior accuracy. The effectiveness of the proposed system is assessed under two different operating conditions. In case 1, the harmonic compensation is analyzed, in which the DVR reduces systemic harmonic disturbances. The results reveal that the proposed controller reduces the total harmonic distortion (THD) from 1.36% to 0.01% while maintaining a constant voltage amplitude of around 0.9986 V, demonstrating strong harmonic suppression capability. Voltage sag mitigation is assessed in Case 2. The load voltage is effectively restored from 0.722 V to 0.9986 V by the DVR, which also reduces THD from 32.97% to 1.6% by injecting the required compensatory current. Overall, the results confirm that the adaptive FOPID–IZA controlled DVR significantly improves power quality and voltage stability in grid-connected systems by effectively mitigating both harmonic distortion and voltage sags.

*This is an open access article under the CC BY-SA license.*

***Corresponding Author:***

Milind Paraye
Department of Electronics and Telecommunication Engineering, Sardar Patel Institute of Technology
University of Mumbai
Andheri, Mumbai, Maharashtra, 400058, India
Email: milind_paraye@spit.ac.in

## 1. INTRODUCTION

Power quality problems, such as voltage sag and harmonic injections, are caused by switching power electronics equipment. When high-sensitivity loads are subjected to such power quality degradation, it can result in significant financial losses for industrial facilities and compromise continuous operation. To address these issues, various equipment and devices are used to enhance power quality. The primary function of these devices is to reduce or completely eradicate the effects of faults that significantly affect the grid performance [1]. According to IEEE Std. 1159-2019, approximately 80–90% of power quality disturbances are attributed to voltage sags, defined as a reduction in root mean square (RMS) voltage from 0.9 p.u. to 0.1 p.u. of nominal voltage [2]. A fault-tolerant control strategy for uncertain nonlinear systems that combines adaptive compensation with active switching to handle actuator and sensor faults. Such fault-tolerant control principles are highly relevant for power-electronic systems, where maintaining load voltage and system

stability under disturbances or device faults is critical [3]. Experts have observed that the deployment of specialty power tools serve as an effective measure to counteract the adverse impacts of electrical disturbances on sensitive distribution system [4]. In the meantime, new technologies such as Dynamic voltage restorers (DVRs) [5], uninterrupted power sources [6], uniform power quality conditioners (UPQC) [7], and active power filters [8]. were introduced. Among these devices the DVR mitigates the impact of voltage sags and swells. This device detects voltage drops in the feeder supplying sensitive loads and injects the appropriate compensating voltage in series through a transformer coupling, thereby mitigating the effects of voltage sags [9]. In real-world scenarios, DVR performance is impacted by random component changes, unmodeled and nonlinear transient behaviour, and imbalanced network problems. Under these circumstances, the classical controllers are distant from operating correctly and are unable to regulate the voltage appropriately [10]. However, the most crucial aspect of this field is creating an appropriate control system. To address this nonlinear and unmodeled transient behaviour and operating point changes, several controllers have been proposed. These include controllers like fuzzy [11], Genetic algorithm (GA) [12] and different control strategies have been employed to adjust the injection voltage to obtain optimal performance, including sliding control [13], robust control [14], and model predictive control (MPC) [15]. Additionally, [16] combined the versatile-based controller and the H∞ controller to enhance performance in both transient and permanent modes. A multilayer inverter with a predictive and optimum control structure was employed [17]. Enhancing the voltage total harmonic distortion (THD) index is also regarded as a crucial goal and a crucial control necessity [18]. Gambôa *et al.* [19], the application of a matrix converter with fly wheel storage is suggested as a solution to the voltage reduction issue. A study on the application of an updated simultaneous reference frame for DVR control may be found in [20]. Apart from resolving power quality concerns in [21], DVR has been employed as a fault current limiter in the event of a load side short circuit.

Despite these developments, a control strategy that can precisely tune parameters, manage nonlinear disturbances, and sustain high performance under a range of sag and harmonic conditions is still required. The integration of fractional-order control with intelligent optimization techniques, especially those that adaptively enhance exploration and exploitation capabilities has not been fully examined in the literature to date. To address this gap, this paper introduces an adaptive fractional order proportional integral derivative (FOPID) controller whose parameters are optimally tuned using an improved zebra algorithm (IZA). Adaptive migration, elite preservation, and dynamic parameter adjustment are all incorporated into the suggested IZA to provide better convergence and increased controller robustness. The suggested DVR control method is a major technical advancement in DVR based power quality control and intelligent optimization because it significantly improves harmonic suppression, voltage recovery, and dynamic stability when combined with the FOPID structure.

## 2. PROPOSED METHOD

### 2.1. Structure of the DVR control system

Distribution systems face challenges in providing stable power to sensitive loads due to harmonic distortion and voltage sags caused by power electronic devices. To address these issues, a system employing a DVR alongside an improved zebra Algorithm-enhanced adaptive FOPID controller is proposed. The DVR stabilizes load voltage by supplying compensatory voltage swiftly, within milliseconds. This study focuses on enhancing DVR control strategies, including components such as series transformers, energy storage systems, and passive filters for harmonic elimination. The FOPID controller is preferred for its superior tuning capabilities, enabling better performance under quickly varying grid conditions, while the IZA optimizes the FOPID parameters for effective voltage sag and harmonic compensation. Figure 1 depicts the proposed setup to eliminate harmonics and voltage issues caused by upstream faults and nonlinearities.

By pumping voltage into DVR through the series transformer into the network, the sensitive load voltage is regulated. Network problems and harmonic loads upstream create harmonic loads or voltages at the point of common coupling (PCC). DVR usually corrects voltage fluctuations. Voltage harmonic removal can be improved in the control system's architecture. Four categories of DVR compensation exist. The first method uses in-phase compensation to match the DVR's voltage injection to the network's voltage after the fault. The second method compensates for pre-sag voltage. This compensatory approach prevents load circulating currents from becoming induced during phase hopping during faults. Energy-minimized voltage compensation, the third method, corrects voltage sag with reactive power. The fourth method, hybrid voltage compensation, combines the prior two. This study uses the second strategy to reach control goals. The (1) uses the DVR circuit model. DVR output filter components are Lf, Cf, and Rf. The transformer includes turns ratio, winding resistance, and inductance $L_t$, while $R_L$and $L_L$ represent load resistance and inductance. A voltage source inverter (VSI) is used to convert the DC-link voltage to AC with the corresponding frequency, phase, and amplitude. This article follows the reference's explanation of VSI switches.

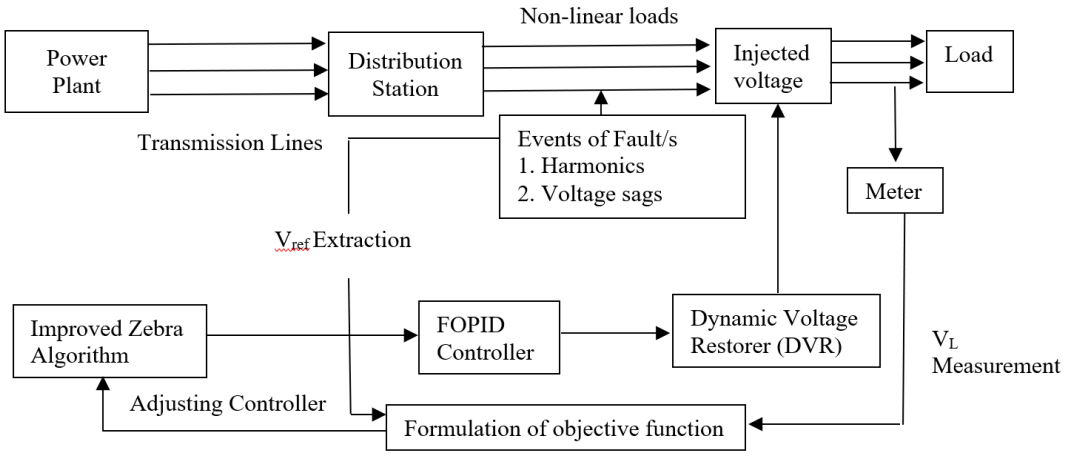


Figure 1. Overview of the DVR control system

$$V_{DVR} = n\left[V_C - n\left(r_t I_t + L_t \frac{dI_t}{dt}\right)\right] \quad (1)$$

The DVR output voltage change rate is actually proportional to the output filter capacitor current, which is how the PCC modifies capacitor current. The dynamic model of the DVR, including line impedance, filter parameters, and transformer dynamics, can be expressed through the following transfer-function polynomials [9]. The (2)-(6) represent this control scheme's transformation function. $K_c$, $k_v$, and $k_{inv}$ are the internal, external, and inverter feedback gains, respectively.

$$v_{load} = G_1 v^*_{load} + G_2 v_{PCC} \quad (2)$$

$$G_1 = \frac{A}{C}, G_2 = \frac{B}{C} \quad (3)$$

$$A = (nk_{inv}k_v k_c + nk_{inv})(L_L s + R_L) \quad (4)$$

$$B = L_L L_f C_f s^3 + \left(L_f R_L + L_L R_f + k_{inv}k_c k_L\right)C_f s^2 + \left(R_f R_L C_f + (1 - nk_{inv})L_L + k_{inv}k_c R_L C_f\right)s + (1 - nk_{inv})R_L \quad (5)$$

$$C = (L_L + n^2 L_t)L_f C_f s^3 + \left[(L_L + n^2 L_t)R_f C_f + (R_L + n^2 R_t)L_f C_f + k_{inv}k_c(L_L + n^2 L_t)C_f\right]s^2 + \left[R_f C_f(R_L + n^2 R_t) + n^2\left(L_f + L_t\right) + L_L(1 + nk_{inv}k_c k_v) + k_{inv}k_c(R_L + n^2 R_t)C_f\right]s + n^2\left(R_f + R_t\right) + R_L(1 + nk_{inv}k_c k_v) \quad (6)$$

The FOPID controller, incorporating fractional calculus to provide greater flexibility and improved performance in control systems (Figure 2).

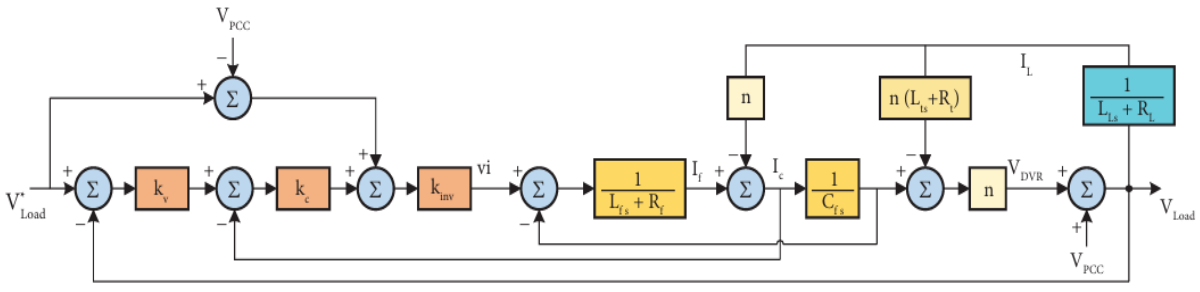


Figure 2. Block diagram of DVR model with closed-loop controller [22]

### 2.2. Objective function formulation

The system's voltage-tracking performance in the dq reference frame was used to establish an objective function that would allow for the best adjustment of the FOPID controller parameters using the IZA. The instantaneous error components were formed by minimizing the difference between the reference voltages ($v_d^{ref}, v_q^{ref}$) and the corresponding load voltages ($v_d^L, v_q^L$).

$$e_d(t) = v_d^{ref}(t) - v_d^L(t), e_q(t) = v_q^{ref}(t) - v_q^L(t) \tag{7}$$

These errors were combined into a single error magnitude:

$$E(t) = \sqrt{e_d^2(t) + e_q^2(t)} \tag{8}$$

To evaluate control performance over time, the Integral Time Absolute Error (ITAE) criterion was used, which penalizes long-duration errors and ensures fast settling:

$$ITAE = \int_0^T t \mid E(t) \mid dt \tag{9}$$

The final optimization objective was to minimize a combined cost function $J$, representing overall tracking performance and dynamic behaviour of the DVR–controller system:

$$J = ITAE = \int_0^T t \sqrt{e_d^2(t) + e_q^2(t)}\, dt \tag{10}$$

This objective function was used by the IZA to select the optimal FOPID control parameters that deliver fast response, minimal steady-state error, and enhanced disturbance compensation.

### 2.3. Optimization of proposed controller parameters with the improved zebra algorithm

In this study, we use the IZA to optimize the DVR system's proportional-derivative (PD) controller's parameters. To guarantee that the closed-loop system offers an appropriate response, the six essential controller parameters—$K_c$, $K_v$, $K_f$, $K_p$, $K_d$, and N—are adjusted.

The first step in the optimization process is to specify the control scheme's goal, which is to reduce the error signal (ES) by (11), which is obtained from the difference of the load voltage and the reference voltage in the dq frame. One way to express the error signal is:

$$ES = \sqrt{\left(V_{ref,d} - V_{L,d}\right)^2 + \left(V_{ref,q} - V_{L,q}\right)^2} \tag{11}$$

where $V_{ref,d}$ and $V_{ref,q}$ are the reference voltages, and $V_{L,d}$ and $V_{L,q}$ are the load voltages in the $d_q$ frame.

The IZA enhances exploration and exploitation capabilities during optimization. The algorithm's exploration phase is responsible for a thorough search of the solution space, avoiding local minima, while the exploitation phase refines the solutions to converge to the optimal parameters. By dynamically modifying its parameters to preserve a balance amongst exploration and exploitation, the IZA's performance is further enhanced.

Through the iterations, the IZA calculates the positions of potential solutions, represented by zebra agents, and updates them based on their cost functions. The final optimized parameters are the parameters that yield the lowest error signal, ensuring the best performance of the DVR system.

In contrast to the conventional metaheuristic methods like particle swarm optimization (PSO) and GA, IZA has the unique strength of balancing exploration and exploitation. Unlike PSO, which tends to converge prematurely, and GA, which entails expensive genetic operations, IZA exploits adaptive migration and elite preservation strategies to ensure diversity and avoid local optima trapping.

### 2.4. Proposed IZA

The IZA enhances the original zebra algorithm (ZA) by addressing issues like premature convergence and performance in high-dimensional spaces. IZA introduces adaptive migration to adjust search step sizes, elite-preservation to retain and amplify the best solutions, and dynamic adjustment of algorithm parameters during iterations. These enhancements improve the balance between exploration and

exploitation, enabling faster convergence, robustness against local minima, and easier tuning of FOPID controller parameters in DVR systems.

Figure 3 illustrates the procedure for optimizing DVR controller parameters using the IZA. First, the DVR system and IZA parameters are initialized, after which random controller gains ($K_c$, $K_v$, $K_F$, $K_p$, $K_d$, λ, μ) are generated to form the initial population. Each parameter set is then evaluated by running a DVR simulation and computing the ITAE objective function, and the best solution with the lowest ITAE is identified. If the maximum iterations are not reached, IZA updates the population using adaptive migration and elite preservation, and the process loops back for further evaluation. Once the iteration limit is met, the optimal parameters are extracted and implemented in the DVR system, where performance is tested under different disturbance cases. If the response meets the required performance criteria, the process ends; otherwise, settings are adjusted, and the optimization is restarted.

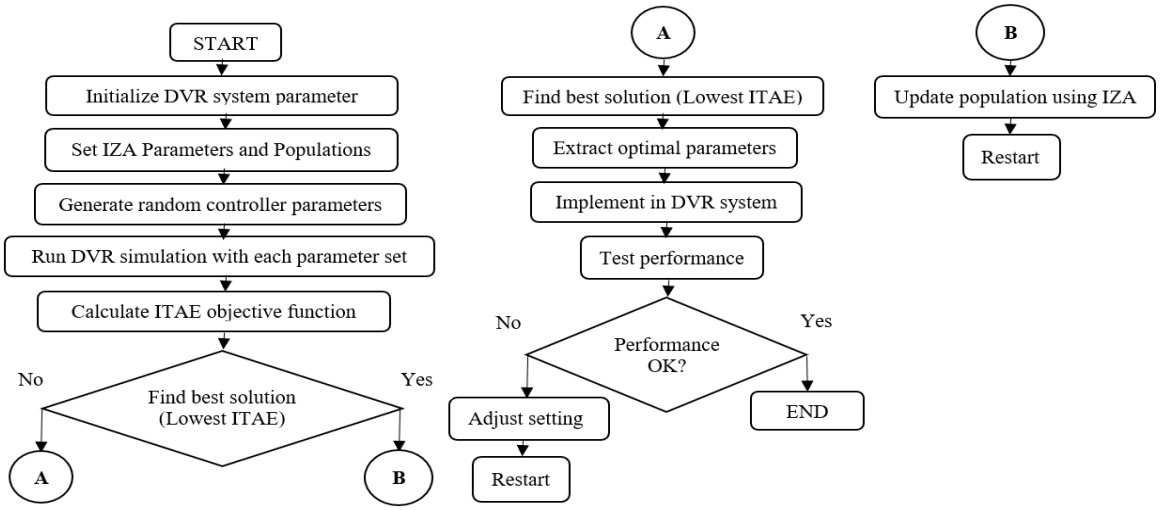


Figure 3. Flowchart of the adaptive FOPID controller optimization using IZA

## 3. RESULTS AND DISCUSSION

### 3.1. Simulation results

As was previously mentioned, the DVR system will be controlled by a closed-loop control arrangement. Due to the complexity of the system, an intelligent optimization algorithm has been selected for implementation that will reduce the chosen objective function (integral time absolute error) to adjust each adaptive control loop parameters, which are "$K_P$, $K_i$ , $K_d$, $\lambda$ and $\mu$". The optimization method that was employed is the improved version of conventional zebra algorithm.

The error response of a control system over time is assessed using the ITAE, a performance index. It minimizes both the duration and magnitude of deviations from the desired output by assigning greater penalties to errors that occur later in time, thereby encouraging faster system settling. This results in smoother system response with reduced oscillations. ITAE is particularly useful for tuning controllers like PID and FOPID, ensuring better stability and performance.

$$ITAE = \int_0^\infty t.|e(t)|dt \tag{12}$$

where, $e(t)$ = error signal (difference between desired and actual output) and t= time

$\int_0^\infty$ = integral over the entire time range

After describing the DVR system, the control problem is formalized in the paper. To improve performance, the optimization algorithm was improved after the control loop parameters were established. Simulations were then carried out, and the resulting data were collected and analyzed. The study concludes by demonstrating the intelligent control structure.

The performance of the proposed DVR controller is evaluated using the distribution system shown in Figure 1 and the variables listed in Table 1. Two scenarios are used for simulations: voltage sag/swell circumstances and normal operation with harmonics. MATLAB is used for all simulations. The DVR specifications are shown in Table 2. The optimized adaptive FOPID tuned parameters are listed in Table 3, the whole distribution system configuration for simulation is shown in Figure 4, and the convergence characteristics of the IZA during parameter tuning are shown in Figure 5.

Table 1. Specifications and parameters of the system

| Network components | Parameter values |
|---|---|
| Load | 400 |
| Transformer | Δ/Y, $R_1$=$R_2$=0.003p.u., $L_1$=$L_2$=0.08p.u., $V_{1(p-p)}$=20kV, $V_{2(p-p)}$=173V, S=50kVA, Delta ($D_1$), Yg (Wye-grounded), 11KV/0,4KV |
| Source | $V_{L-L}$=20kV, f=60Hz |
| Nominal frequency (Hz) | 50 |
| Active power P (W) | 1.5e3 |
| Inductive reactive power QL (positive var) | 100 |
| Capacitive reactive power Qc (negative var) | 0 |

Table 2. DVR specifications

| Parameters | Values |
|---|---|
| Series transformer | S =1.5e3 VA, $V_1$=10V, $V_2$ = 100V, $R_1$= $R_2$ = 0.0003 pu, $X_1$ =$X_2$ =200 pu |
| Energy source voltage | 200V |
| Output filter of the inverter | C=20e-6, L=6e-3 |
| Switching frequency | 50 Hz, |
| Adaptive notch filter (ANF) | c = 10000, $\zeta_1$ =0.2, $\zeta_{5,7}$ = 0.8 |

Table 3. Adaptive FOPID tuned parameters

| Parameters | $K_p$ | $K_i$ | $\lambda$ | $\mu$ | $\gamma$ |
|---|---|---|---|---|---|
| Value | 40 | 154 | 0.5 | 0.7 | -0.5 |

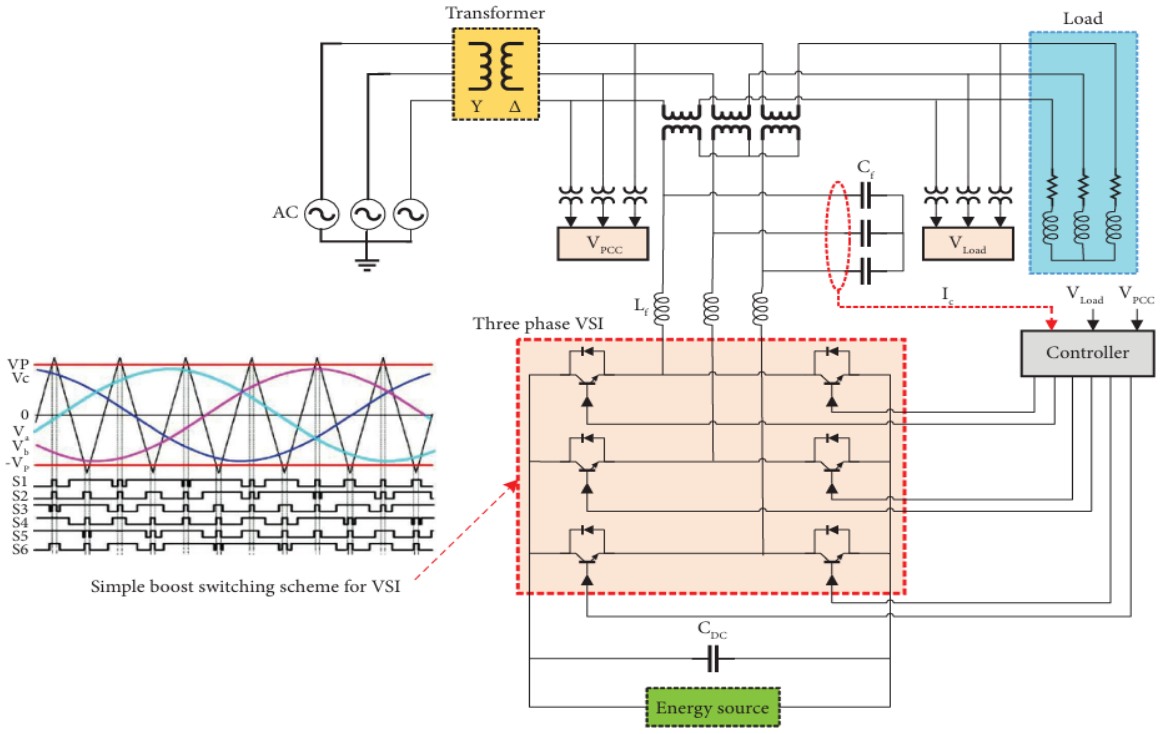


Figure 4. The system under study [22]

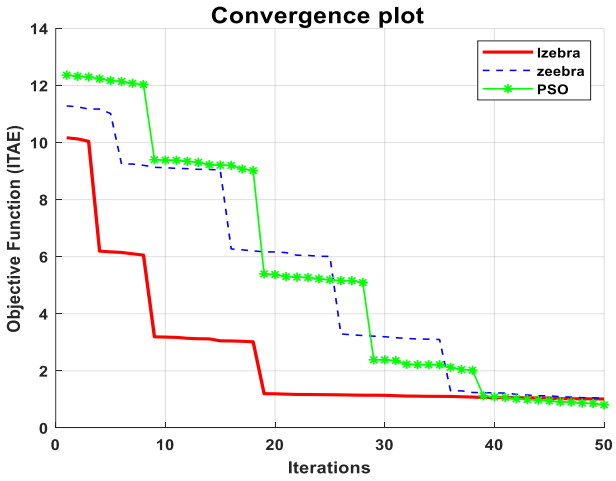


Figure 5. Convergence plot

### 3.1.1. Case 1

In this case, the proposed adaptive FOPID controller for the DVR is used to evaluate harmonic compensation. As mentioned earlier, voltage sags occur less frequently in power networks compared to harmonic disturbances. Therefore, implementing a DVR solely for mitigating voltage sags may not always be economically justified. Figures 6 and 7 show the reference voltage, load voltage, injected voltage, and the voltage at the transformer secondary terminals obtained from simulation results. The DVR injects the required compensating voltage into the network, enabling the load to receive voltage with minimal harmonic distortion. For further analysis, Figure 8 illustrates the THD (%) of phase voltages at the PCC and the load. After DVR compensation, the voltage THD decreases significantly from 1.36% to 0.01%.

The voltage amplitude and THD values prior to and following harmonic adjustment utilizing the DVR with the adaptive FOPID controller are compiled in Table 4. The voltage amplitudes before and after compensation are shown in Figures 6 and 7, illustrating how well the DVR reduces harmonic distortion. Phases Va, Vb, and Vc experience a modest increase in voltage amplitude from 0.9922 V to 0.9986 V. THD is dramatically decreased, as seen in Figure 8, going from 1.36%, 1.46%, and 1.52% to 0.01% for all phases following compensation.

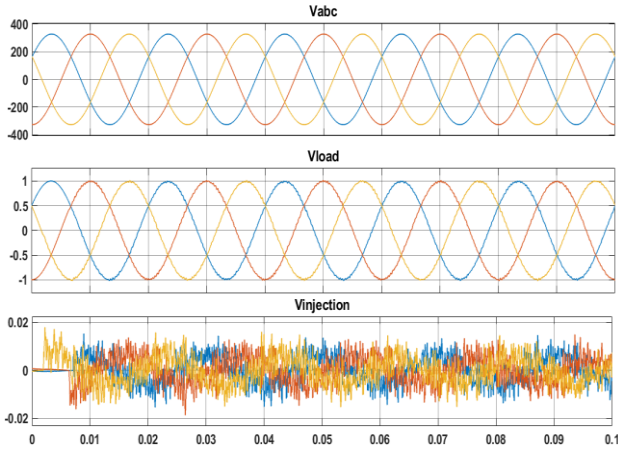


Figure 6. Voltage amplitude before harmonic compensation

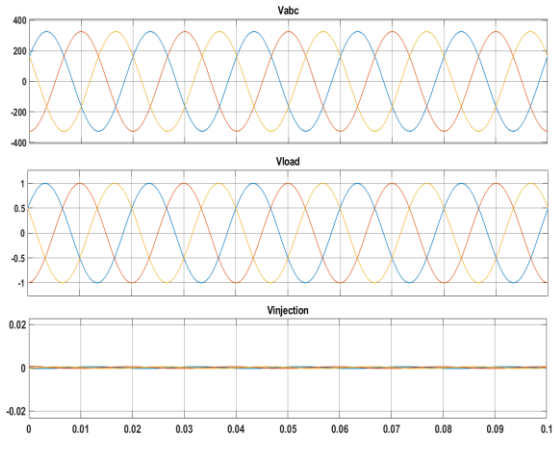


Figure 7. Voltage amplitude after harmonic compensation

### 3.1.2. Case 2

In this instance, a voltage sag occurs between 0.03 and 0.07 seconds due to the application of a three-phase fault. The load voltage, injected voltage, and voltage at the transformer secondary terminals are shown in

Figures 9 and 10. The findings verify that the DVR injects the necessary compensating voltage during the failure, enabling the load voltage to fall apart when maintained with the least amount of harmonic distortion.

By contrasting the system's effectiveness with and without the DVR, Table 5 provides an overview of the voltage amplitude and THD values for Case 2. The voltage amplitude across phases Va, Vb, and Vc decreases to approximately 0.722 V in the absence of the DVR, with extremely high THD values of 32.97%, 39.23%, and 32.61%, respectively. Figure 9 depicts the voltage amplitude without the DVR, while Figure 10 shows the improved voltage amplitude following DVR installation. Following DVR implementation, the voltage amplitude increases significantly to approximately 0.9986 V for all phases, while THD decreases to 1.61%, 1.80%, and 1.73% for phases Va, Vb, and Vc. The THD % for the two scenarios are contrasted in Figure 11, demonstrating how well the DVR reduces harmonic distortion.

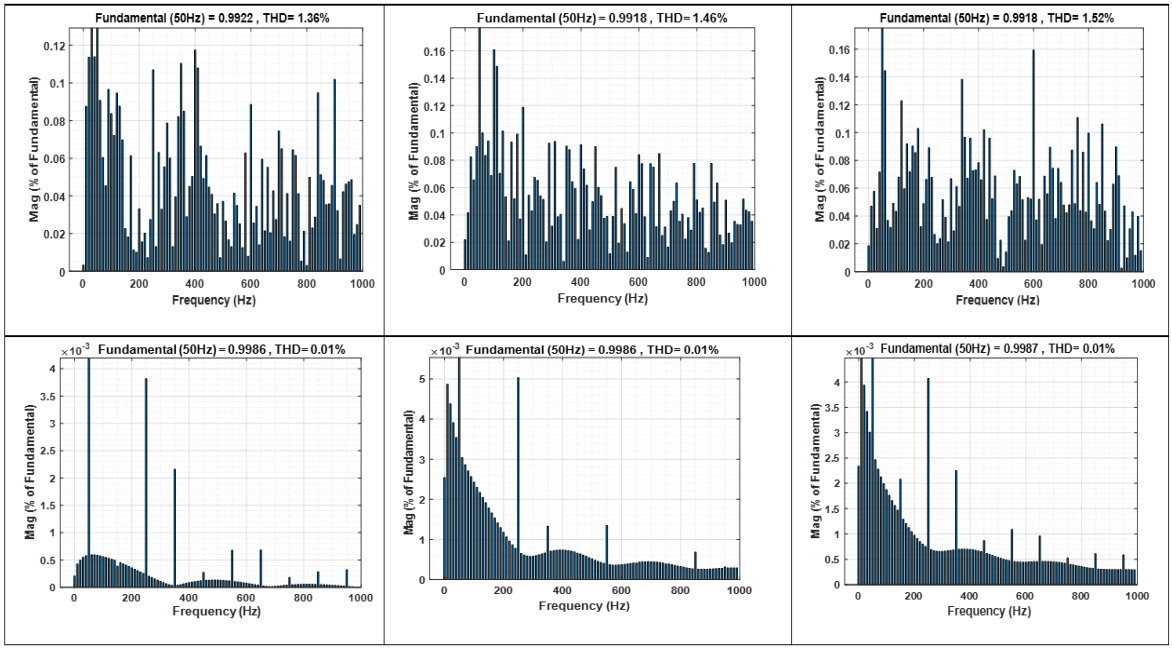


Figure 8. THD % before and after harmonic compensation

Table 4. Summary of the results of case 1

| Voltage phase | Before harmonic compensation | | After harmonic compensation | |
|---|---|---|---|---|
| | Voltage (V) | THD (%) | Voltage (V) | THD (%) |
| Va | 0.9922 | 1.36 | 0.9986 | 0.01 |
| Vb | 0.9918 | 1.46 | 0.9986 | 0.01 |
| Vc | 0.9918 | 1.52 | 0.9987 | 0.01 |

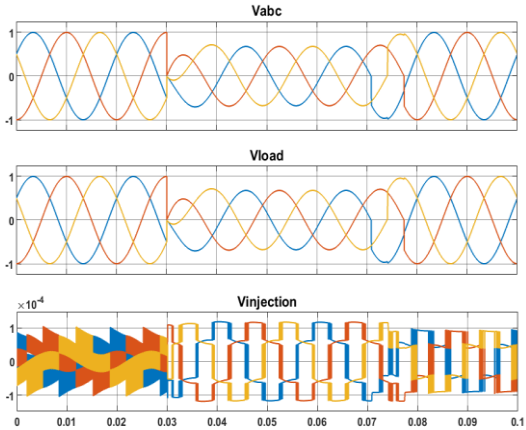


Figure 9. Voltage amplitude (V) in without DVR

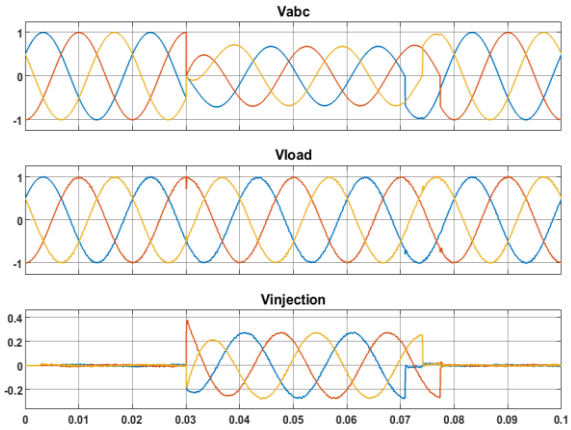


Figure 10. Voltage amplitude (V) with DVR

Table 5. Summary of the results of case 2

| Voltage phase | Without DVR | | With DVR | |
|---|---|---|---|---|
| | Voltage (V) | THD (%) | Voltage (V) | THD (%) |
| Va | 0.722 | 32.97 | 0.9986 | 1.61 |
| Vb | 0.718 | 39.23 | 0.9986 | 1.80 |
| Vc | 0.719 | 32.61 | 0.9987 | 1.73 |

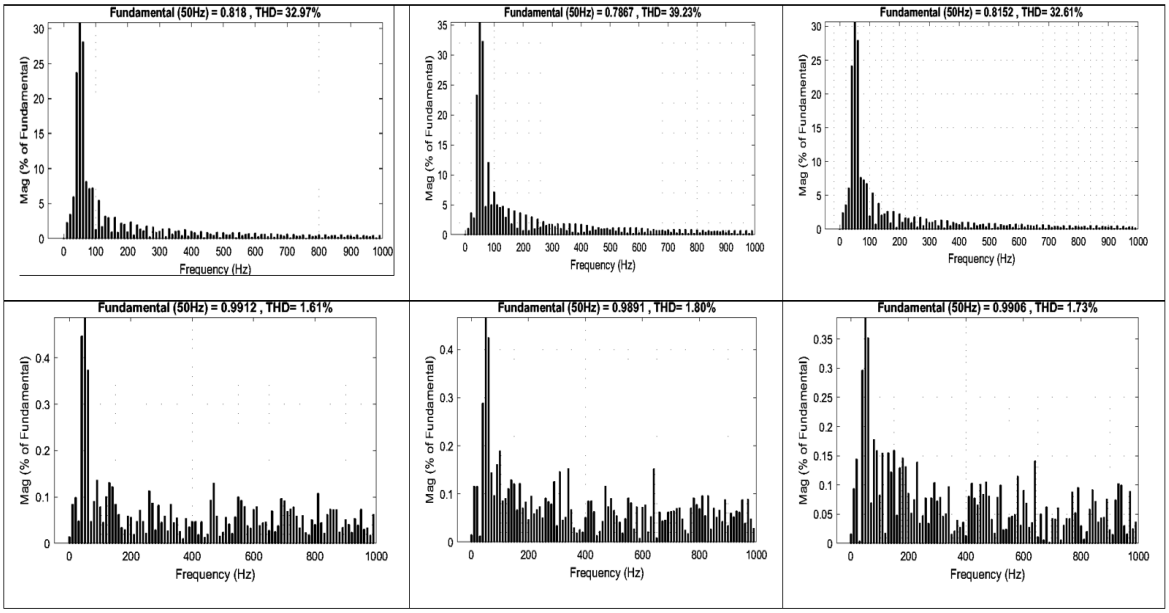


Figure 11. THD% with and without DVR cases

Figure 12 shows set of convergence plots illustrating the performance of four optimization algorithms—IZA, PSO, GA, and Pufferfish—on six benchmark functions: Rosenbrock, Rastrigin, Step, Zakharov, Ackley, and Griewank functions. Each plot represents how the fitness value decreases over 200 iterations, indicating the convergence behavior of the algorithms toward an optimal solution. The number of iterations is shown on the x-axis, while the fitness value is shown on the y-axis. The stepwise decline in fitness values suggests the progressive improvement of solutions over time. Among the algorithms, IZA consistently shows a faster convergence rate with lower final fitness values, followed by PSO, GA, and Pufferfish. These plots are essential for evaluating the efficiency of optimization algorithms in solving complex mathematical functions.

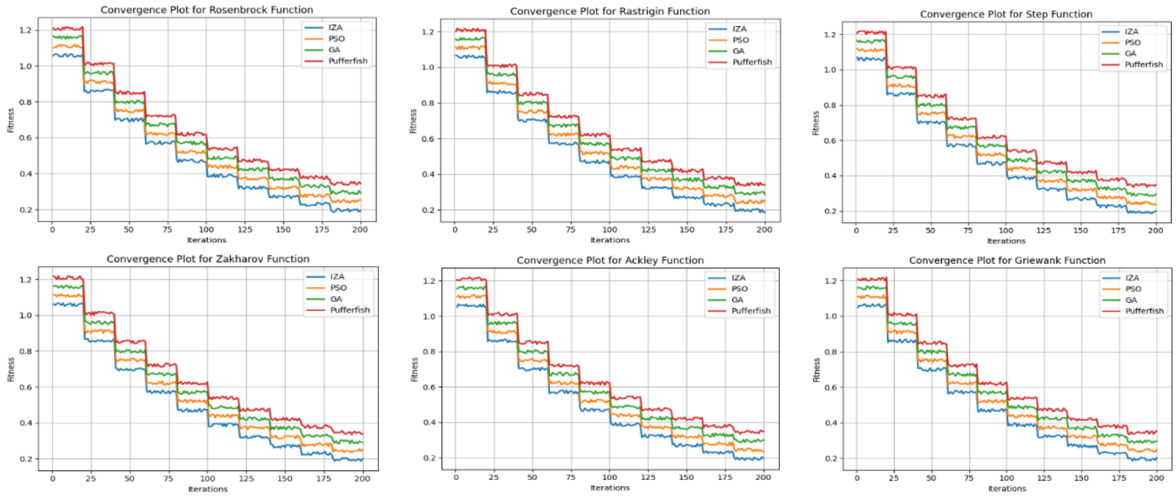


Figure 12. Comparison of algorithms

### 3.2. Discussion

The simulation results showed that the DVR with the adaptive FOPID controller greatly improved voltage stability and harmonic mitigation in both normal and fault-disturbed situations. Before compensation in Case 1, the voltage amplitudes of phases Va, Vb, and Vc were about 0.992 V, and the THD values were 1.36%, 1.46%, and 1.52%. After activating the DVR, the THD dropped sharply to 0.01% for all phases, and the voltage amplitude rose to 0.9986 V. Figures 6, 7, and 8 show these results. They show that the controller made it possible to inject voltage very accurately and almost completely block harmonic components. The enhancement validates that the integration of fractional-order control and intelligent optimization resulted in a markedly superior response relative to traditional methods.

The suggested approach is directly compared to prominent optimization-based and sophisticated control strategies that have been documented in the literature in Table 6. This aids in placing the suggested approach within the framework of current DVR research. The results clearly show that the proposed DVR–adaptive FOPID controller had lower THD levels after compensation than the Black Widow Optimization + FOPID [23], water cycle algorithm–based tuning [24], and feedforward + active disturbance rejection control (ADRC) [25] methods, even though they made significant improvements. The IZA's ability to tune is shown by the very low THD of 0.01% in case 1 and the big drop that happens during sag conditions.

Further analysis of Case 2 revealed that the proposed controller effectively managed severe conditions during a three-phase fault. Without the DVR, voltage dropped to approximately 0.722 V with a high THD of around 32.97% for Va. With the DVR activated, voltage improved to 0.9986 V and THD reduced to around 1.61%. This highlights the DVR's crucial role in stabilizing voltage and minimizing harmonic distortion during faults. The IZA-optimized adaptive FOPID controller demonstrates significant reliability and responsiveness, making it a promising solution as power distribution systems evolve with more nonlinear loads and renewable resources. Future research aims to validate the framework with hardware testing and optimize it further, potentially increasing the controller's adaptability and performance in handling disturbances. The DVR-enhanced FOPID framework shows strong capabilities in harmonic suppression and voltage recovery, contributing positively to power quality advancements.

Table 6. Comparative analysis

| No. | Reference (controller and method) | Pre-DVR THD/Voltage | Post-DVR THD/Voltage |
|---|---|---|---|
| 1 | Black Widow Optimization + FOPID [23] | Not explicitly stated | Effective harmonic compensation observed, overshoot ~2.9 %, undershoot ~5.6 %, settling ≈0.104 s |
| 2 | Study using water cycle algorithm for DVR (PID/PI/FOPI/FOPID, CSSE) [24] | THDPI ≈1.61 %, THDPID ≈0.71 %, THDFOPI ≈1.60 %, THDFOPID ≈1.20 % | FOPID yielded THD ≈1.20 % in balanced sags; other controllers slightly higher |
| 3 | Feed-forward + ADRC control [25] | Traditional PI control THD ≈2.49 % | THD ≈1.43 % |
| 4 | Proposed method | Case1 : THD =1.36% Case 2: THD=32.61% | THD = 0.01% THD= 1.61% |

## 4. CONCLUSION

This study showed that the IZA-optimized adaptive FOPID controller made the DVR work much better in grid-connected settings. The proposed control framework showed that it could adapt faster, reject disturbances better, and regulate voltage more accurately than traditional DVR methods. The controller kept the load voltage stable and effectively made up for harmonic distortions and voltage sags in a variety of operating situations. This shows that it is good for networks with nonlinear loads and changing operating conditions. The IZA-optimized adaptive FOPID controller made the system more stable and supported higher power quality standards by making it easier to tune parameters and improving dynamic response. The results indicate that the proposed method performs effectively for next-generation DVRs, particularly in distribution networks with renewable energy integration and sensitive electronic equipment. Future research might build on this work by including real-time digital controller implementation, hardware-in-the-loop testing, and hybrid optimization techniques to increase computational efficiency and dependability.

**FUNDING INFORMATION**

The authors declare that no funding was received for the conduct of this study.

## AUTHOR CONTRIBUTIONS STATEMENT

This journal uses the Contributor Roles Taxonomy (CRediT) to recognize individual author contributions, reduce authorship disputes, and facilitate collaboration.

| Name of Author | C | M | So | Va | Fo | I | R | D | O | E | Vi | Su | P | Fu |
|---|---|---|---|---|---|---|---|---|---|---|---|---|---|---|
| Milind Paraye | ✓ | ✓ | ✓ | ✓ | ✓ | ✓ | | ✓ | ✓ | ✓ | | | ✓ | |
| Rajendra G. Sutar | ✓ | ✓ | ✓ | ✓ | | | ✓ | | ✓ | | | ✓ | | |

C : **C**onceptualization
M : **M**ethodology
So : **So**ftware
Va : **Va**lidation
Fo : **Fo**rmal analysis
I : **I**nvestigation
R : **R**esources
D : **D**ata Curation
O : Writing - **O**riginal Draft
E : Writing - Review & **E**diting
Vi : **Vi**sualization
Su : **Su**pervision
P : **P**roject administration
Fu : **Fu**nding acquisition

## CONFLICT OF INTEREST STATEMENT

The authors state no conflict of interest.

## DATA AVAILABILITY

Data availability does not apply to this paper as no new data were created or analyzed in this study.

## REFERENCES


[1] A. H. Soomro, A. S. Larik, M. A. Mahar, A. A. Sahito, A. M. Soomro, and G. S. Kaloi, "Dynamic voltage restorer—a comprehensive review," *Energy Reports*, vol. 7, pp. 6786–6805, Nov. 2021, doi: 10.1016/j.egyr.2021.09.004.

[2] X. Xie and Y. Sun, "A piecewise probabilistic harmonic power flow approach in unbalanced residential distribution systems," *International Journal of Electrical Power & Energy Systems*, vol. 141, p. 108114, Oct. 2022, doi: 10.1016/j.ijepes.2022.108114.

[3] X. Yang, X. Wang, S. Wang, and V. Puig, "Switching-based adaptive fault-tolerant control for uncertain nonlinear systems against actuator and sensor faults," *Journal of the Franklin Institute*, vol. 360, no. 16, pp. 11462–11488, Nov. 2023, doi: 10.1016/j.jfranklin.2023.08.042.

[4] V. Vinothkumar and R. Kanimozhi, "Recent trends in power quality improvement using custom power devices and its performance analysis," *Turkish Journal of Computer and Mathematics Education*, vol. 12, no. 7, pp. 1686–1694, 2021.

[5] N. Abas, S. Dilshad, A. Khalid, M. S. Saleem, and N. Khan, "Power quality improvement using dynamic voltage restorer," *IEEE Access*, vol. 8, pp. 164325–164339, 2020, doi: 10.1109/ACCESS.2020.3022477.

[6] Y. Naderi, S. H. Hosseini, S. Ghassem Zadeh, B. Mohammadi-Ivatloo, J. C. Vasquez, and J. M. Guerrero, "An overview of power quality enhancement techniques applied to distributed generation in electrical distribution networks," *Renewable and Sustainable Energy Reviews*, vol. 93, pp. 201–214, Oct. 2018, doi: 10.1016/j.rser.2018.05.013.

[7] S. S. Bhosale, Y. N. Bhosale, U. M. Chavan, and S. A. Malvekar, "Power quality improvement by using UPQC: a review," in *2018 International Conference on Control, Power, Communication and Computing Technologies (ICCPCCT)*, IEEE, Mar. 2018, pp. 375–380. doi: 10.1109/ICCPCCT.2018.8574264.

[8] C. Yang, Z. Wu, X. Li, and A. Fars, "Risk-constrained stochastic scheduling for energy hub: integrating renewables, demand response, and electric vehicles," *Energy*, vol. 288, p. 129680, Feb. 2024, doi: 10.1016/j.energy.2023.129680.

[9] A. Ghosh and G. Ledwich, "Compensation of distribution system voltage using DVR," *IEEE Transactions on Power Delivery*, vol. 17, no. 4, pp. 1030–1036, Oct. 2002, doi: 10.1109/TPWRD.2002.803839.

[10] A. Moghassemi and S. Padmanaban, "Dynamic voltage restorer (DVR): a comprehensive review of topologies, power converters, control methods, and modified configurations," *Energies*, vol. 13, no. 16, p. 4152, Aug. 2020, doi: 10.3390/en13164152.

[11] S. R. Arya, K. D. Mistry, and P. Kumar, "A hybrid fuzzy predictive DVR model for voltage estimation using intelligent learning," *IEEE Transactions on Power Delivery*, vol. 39, no. 1, pp. 378–385, Feb. 2024, doi: 10.1109/TPWRD.2022.3227216.

[12] S. Zhou, G. Zhou, M. He, S. Mao, H. Zhao, and G. Liu, "Stability effect of different modulation parameters in voltage-mode PWM control for CCM switching DC–DC converter," *IEEE Transactions on Transportation Electrification*, vol. 10, no. 2, pp. 2408–2422, Jun. 2024, doi: 10.1109/TTE.2023.3293811.

[13] H. Ahmed, S. Biricik, H. Komurcugil, S. Ben Elghali, and M. Benbouzid, "Enhanced frequency-adaptive self-tuning filter-based continuous terminal sliding mode control of single-phase dynamic voltage restorer," *Control Engineering Practice*, vol. 128, p. 105340, Nov. 2022, doi: 10.1016/j.conengprac.2022.105340.

[14] S. DaneshvarDehnavi, C. Negri, S. Bayne, and M. Giesselmann, "Dynamic voltage restorer (DVR) with a novel robust control strategy," *ISA Transactions*, vol. 121, pp. 316–326, Feb. 2022, doi: 10.1016/j.isatra.2021.04.010.

[15] M. Dashtdar *et al.*, "Frequency control of the islanded microgrid based on optimised model predictive control by PSO," *IET Renewable Power Generation*, vol. 16, no. 10, pp. 2088–2100, Jul. 2022, doi: 10.1049/rpg2.12492.

[16] J. Zhao and L. Mili, "A theoretical framework of robust H-infinity unscented Kalman filter and its application to power system dynamic state estimation," *IEEE Transactions on Signal Processing*, vol. 67, no. 10, pp. 2734–2746, May 2019, doi: 10.1109/TSP.2019.2908910.

[17] A. C. Kathiresan, P. R. Jeyaraj, B. K. Albert, S. B. Thanikanti, M. K. Nallapaneni, and H. H. Alhelou, "A versatile control of solar DVR for enhanced utilization and power quality improvement in a series-connected wind-solar farm," *IET Renewable Power Generation*, vol. 19, p. e12592, Jan. 2025, doi: 10.1049/rpg2.12592.

[18] M. R. Khalghani and M. H. Khooban, "A novel self-tuning control method based on regulated bi-objective emotional learning controller's structure with TLBO algorithm to control DVR compensator," *Applied Soft Computing*, vol. 24, pp. 912–922, Nov. 2014, doi: 10.1016/j.asoc.2014.08.051.

[19] P. Gambôa, J. F. Silva, S. F. Pinto, and E. Margato, "Input–output linearization and PI controllers for AC–AC matrix converter based dynamic voltage restorers with flywheel energy storage: a comparison," *Electric Power Systems Research*, vol. 169, pp. 214–228, Apr. 2019, doi: 10.1016/j.epsr.2018.12.023.
[20] F. B. Moreno, J. E. Palacios, J. Posada, and J. A. Lopez, "Implementation and evaluation of a new DVR topology with AC link for series compensation," *Electric Power Systems Research*, vol. 181, p. 106184, Apr. 2020, doi: 10.1016/j.epsr.2019.106184.
[21] P. Ghavidel, M. Farhadi, M. Dabbaghjamanesh, A. Jolfaei, and M. Sabahi, "Fault current limiter dynamic voltage restorer (FCL-DVR) with reduced number of components," *IEEE Journal of Emerging and Selected Topics in Industrial Electronics*, vol. 2, no. 4, pp. 526–534, Oct. 2021, doi: 10.1109/JESTIE.2021.3051586.
[22] M. M. Alrashed, A. Flah, M. Dashtdar, C. Z. El-Bayeh, and M. F. Elnaggar, "Improving the control strategy of the DVR compensator based on an adaptive notch filter with an optimized PD controller using the IGWO algorithm," *International Transactions on Electrical Energy Systems*, vol. 2024, p. 5097056, Jan. 2024, doi: 10.1155/2024/5097056.
[23] B. Srikanth Goud *et al.*, "Dynamic voltage restorer to mitigate voltage sag/swell using black widow optimization technique with FOPID controller," *EAI Endorsed Transactions on Energy Web*, vol. 10, Nov. 2023, doi: 10.4108/ew.4331.
[24] T. Thongsan and T. Chatchanayuenyong, "Optimal dynamic voltage restorer using water cycle optimization algorithm," *Computer Systems Science and Engineering*, vol. 45, no. 1, pp. 595–623, 2023, doi: 10.32604/csse.2023.027966.
[25] L. Huang, W. Liu, N. Zhang, Q. Yan, and X. Wei, "Modulation strategy of dynamic voltage restorer based on dual-feedforward active disturbance rejection compound controller," *Frontiers in Energy Research*, vol. 12, p. 1462565, Jan. 2025, doi: 10.3389/fenrg.2024.1462565.

## BIOGRAPHIES OF AUTHORS

**Milind Paraye** received his master degree in Electronics Engineering from the University of Mumbai, in 2013. He is a Ph.D. student at Sardar Patel Institute of Technology, University of Mumbai since 2020. His current interests include smart grid simulation and optimization, power quality, and artificial neural network implementation. He can be contacted at email: milind_paraye@spit.ac.in.

**Dr. Rajendra G. Sutar** received B.E. degree in Electronics Engineering from Shivaji University, Kolhapur, India, M.E. degree in Electronics Engineering from Mumbai University, Mumbai, India, and Ph.D. degree from V.N.I.T. Nagpur, India. He is a senior member of IEEE. He is working as an Associate Professor in the Department of Electronics and Telecommunication Engineering, Sardar Patel Institute of Technology, Andheri (West), Mumbai, India. His research interests include biomedical electronics, biomedical signal processing, and power electronic circuits and systems. He can be contacted at email: rajendra_sutar@spit.ac.in.